

Statistical approach to quantifying the elastic deformation of nanomaterials

Xinwei Deng^a, V. Roshan Joseph^a, Wenjie Mai^b, Zhong Lin Wang^b, and C. F. Jeff Wu^{a,1}

^aH. Milton Stewart School of Industrial and Systems Engineering and ^bSchool of Materials Science and Engineering, Georgia Institute of Technology, Atlanta GA 30332

Edited by Peter J. Bickel, University of California, Berkeley, CA, and approved April 22, 2009 (received for review September 3, 2008)

Quantifying the mechanical properties of nanomaterials is challenged by its small size, difficulty of manipulation, lack of reliable measurement techniques, and grossly varying measurement conditions and environment. A recently proposed approach is to estimate the elastic modulus from a force-deflection physical model based on the continuous bridged-deformation of a nanobelt/nanowire using an atomic force microscope tip under different contact forces. However, the nanobelt may have some initial bending, surface roughness and imperfect physical boundary conditions during measurement, leading to large systematic errors and uncertainty in data quantification. In this article, a statistical modeling technique, sequential profile adjustment by regression (SPAR), is proposed to account for and eliminate the various experimental errors and artifacts. SPAR can automatically detect and remove the systematic errors and therefore gives more precise estimation of the elastic modulus. This research presents an innovative approach that can potentially have a broad impact in quantitative nanomechanics and nanoelectronics.

model selection | nanomechanics | nanostructure | profile adjustment | regression modeling

Nanotechnology has provided unprecedented understanding and applications on materials and is impacting many fields through the development of nanodevices and nanosystems that exhibit superior performances. The fundamental building blocks in constructing such devices and systems are 1-dimensional (1D) nanomaterials, such as carbon nanotubes, semiconductor nanowires, and oxide nanobelts. The mechanical behavior of 1D nanomaterials is one of most important properties dictating their applications in nanotechnology. Among the several developed methods for measuring the elastic deformation properties of nanomaterials (1–3), one approach to quantifying the elastic modulus of 1D nanomaterials is based on the atomic force microscopy (AFM). A common strategy is to deform a 1D nanostructure using an AFM tip, which pushes the 1D nanostructure at some locations. Then the elastic modulus is determined through quantifying the force-displacement curve. The accuracy of this measurement is, however, limited by noise factors such as the size of the tip, the accuracy of positioning the AFM tip on the object, the surface roughness of the 1D nanomaterials, and the stability of the structure during measurements. New approaches are needed for analyzing the data received from nano-scale measurements, so that the derived information can be reliably used to characterize the mechanical properties of nanomaterials. The objective of this article is to propose a new approach for quantitative nanomechanics through statistical and physical modeling.

Recently, Mai and Wang (4) proposed a new approach for quantifying the elastic deformation behavior of 1D nanostructures. The approach is based on a continuous deformation/bending of a Zinc Oxide (ZnO) nanobelt/nanowire, which is supported at its two ends by a trenched substrate, using an AFM tip in contact mode. The AFM tip scans along the length of the nanobelt under a constant applied force, and thus the segment across the trench is deformed. A quantitative fitting of the force-deflection curve is used for estimating the elastic modulus of the nanobelt. However,

the measured data are largely affected by the imperfect shape of the nanobelt, its surface roughness, size and shape of the AFM tip, and the instability of the measurement technique at such a small scale. Moreover, the level of allowable tolerance on measurement errors for the nanomaterials decreases because noise or error becomes much larger compared with the small response signals from the nanomaterials. The data analysis is complicated by a lack of confidence in the assumed physical model to accommodate the uncertainty in the contact between the nanobelt and the supporting trench. One possible physical model is the simply-supported beam model (SSBM) (5). The SSBM is an ideal case that does not account for the various experimental uncertainties and artifacts. In this article, we use an empirical statistical modeling technique to identify the effects of these artifacts and their influence on data analysis. After filtering out such effects, we can accurately, reliably and efficiently determine the elastic modulus based on the physical law. Our study sets a good and early example for quantitative nanomechanics. The proposed methodology can be extended to other fields in nanotechnology such as nanoelectronics and nanomeasurements.

Existing Method

Mai and Wang (4) used a physical vapor deposition method to synthesize the ZnO nanobelts with a rectangular cross-section. A silicon substrate was prepared with long and parallel trenches carved at its surface by nanofabrication. The trenches are ≈ 200 nm deep and $1.25 \mu\text{m}$ wide. They manipulated the long ZnO nanobelts across the trenches over many periods. A scanning electron microscopy (SEM) and AFM were used to capture the morphology and dimensions of the nanobelt. The length and width of the nanobelt are captured by the SEM image and the thickness of the nanobelt is obtained from AFM image. In the mechanical measurement, an AFM tip scanned the nanobelt along its length direction in contact mode at a constant applied force. By changing the magnitude of the contact force from low to high, they obtained a series of bending profiles of the nanobelt.

The profiles of a suspended nanobelt along the length direction under different contact forces are shown in Fig. 1A. As shown in Fig. 1A, the image profiles of a nanobelt (denoted by NB) recorded the deflection of all of the points along its length under different applied forces. Each curve was obtained by averaging 10 consecutive measurements along its length under the same loading force. The curves in Fig. 1A are not smooth because of a small surface roughness (≈ 1 nm) of the nanobelt. In addition, the as-attached nanobelt on the trenches is not perfectly straight, possibly because of initial bending during the sample manipulation. Fig. 1A indicates that there are some noise factors affecting the deflection curves. To eliminate the effect of the surface roughness and initial bending of the nanobelt (collectively referred to as initial bias), Mai and Wang

Author contributions: X.D., R.J., Z.L.W., and C.F.J.W. designed research; X.D., R.J., W.M., and C.F.J.W. performed research; X.D. analyzed data; and X.D., R.J., and C.F.J.W. wrote the paper.

The authors declare no conflict of interest.

This article is a PNAS Direct Submission.

¹To whom correspondence should be addressed. E-mail: jeffwu@isye.gatech.edu.

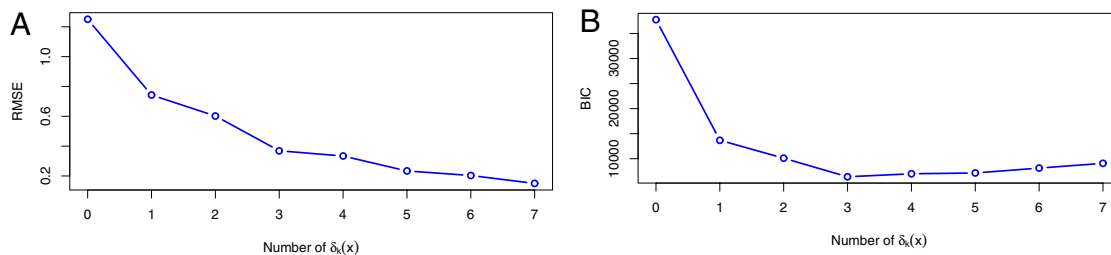


Fig. 4. Forward model selection using RMSE and BIC on the NB data.

increase with force. The SSBM itself cannot explain this phenomenon. One possible explanation is the change of the boundary conditions, which can be nonlinear and irreversible during the measurement. This pattern still persists in the normalized profiles in Fig. 1B. Therefore, the MW method cannot be used to fit the profile data properly. It requires a more general model to identify other factors besides the initial bias.

To overcome these problems, we propose a physical-statistical model that integrates SSBM with a regression model. The regression model captures the initial bias and potential systematic biases introduced during measurement. We use model selection to identify terms associated with the systematic biases and adjust the

profiles by subtracting these terms from the original profiles. This provides a better estimate of the elastic modulus E . We call the method sequential profile adjustment by regression (SPAR).

General Model and Model Selection

General Model. As shown in Fig. 1A, suppose there are K image profiles, i.e., the nanobelt is scanned sequentially under K different applied forces F_1, F_2, \dots, F_K . The experimenter usually changes the magnitude of applied force F from low to high, i.e., $F_1 < F_2 < \dots < F_K$. Each profile contains n points, which are recorded at the distances of x_1, x_2, \dots, x_n . We denote the deflection at the distance x under the applied force F as $v(x, F)$. Then the SSBM can be written as

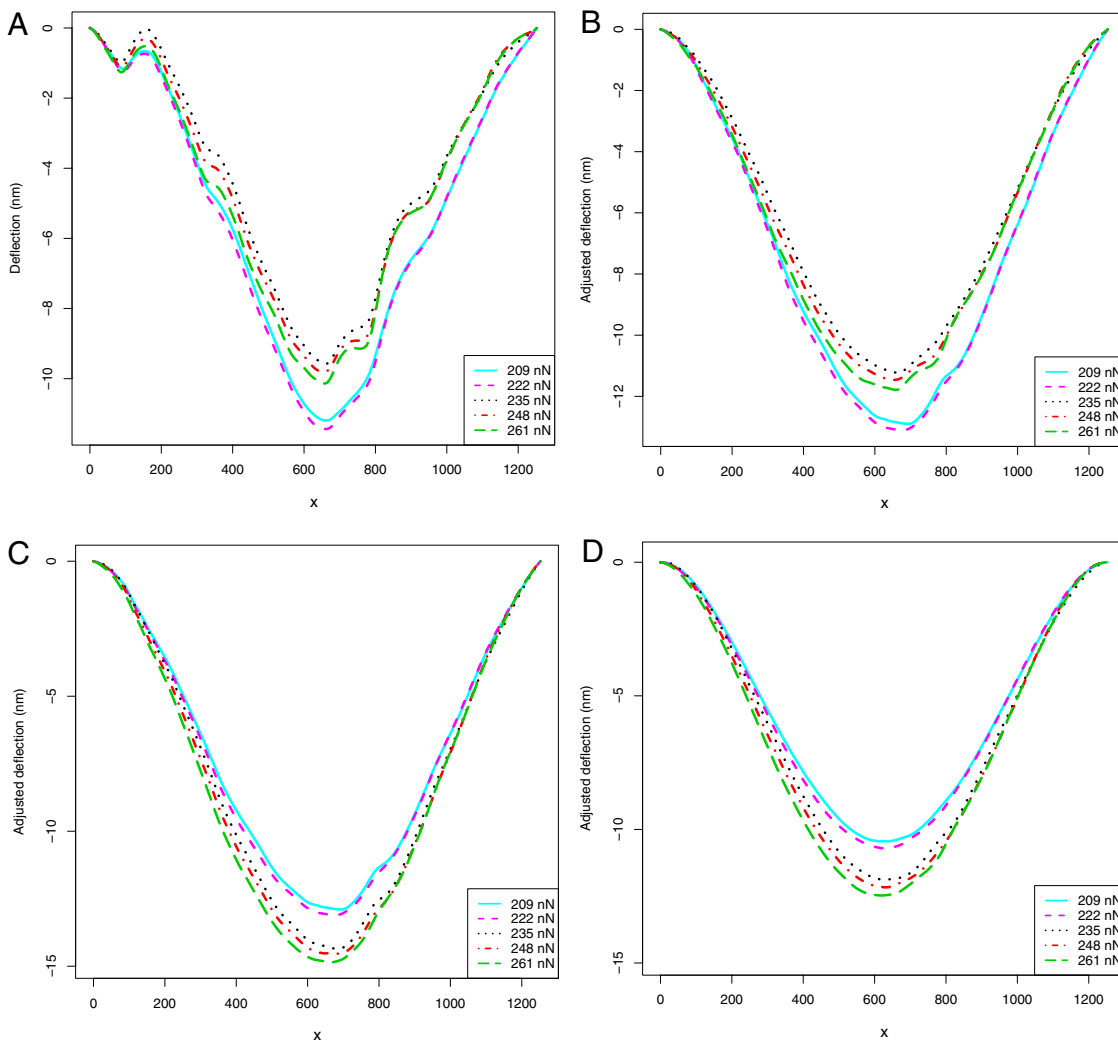


Fig. 5. Illustration of the adjusted deflection profiles under applied force from $F_{11} = 209$ nN to $F_{15} = 261$ nN.

Table 1. Comparison of estimates with the NB data

	RMSE	1/E	se(1/E)	\hat{E} , GPa	se(E)
MW method	0.86	1.06×10^{-2}	1.77×10^{-4}	94.34	1.58
SPAR	0.37	9.85×10^{-3}	7.63×10^{-5}	101.52	0.79

$$\text{BIC} = \sum_{i=1}^n \sum_{k=1}^K (v(x_i, F_k) - \hat{v}(x_i, F_k))^2 / \sigma^2 + p \log N. \quad [6]$$

Here, p is the number of parameters, and N is the number of observations in the corresponding regression model. If σ^2 in Eq. 6 is not available, an estimate $\hat{\sigma}^2$ can be obtained from the replicates. The R code for implementing the SPAR method is available from the authors upon request.

Example. In the image profiles of the nanobelt, the deflection is recorded at $n = 161$ points along the length of the nanobelt under $K = 15$ different applied forces. The length of NB is $L = 1,252$ nm and the moment of inertia in the SSBM is $I = 8,216,510 \text{ nm}^4$. Fig. 4 shows the model selection results obtained using the proposed method. The $\delta_k(x)$ is sequentially selected into the model in the following order: $\delta_0(x)$, $\delta_{12}(x)$, $\delta_{10}(x)$, $\delta_8(x)$, $\delta_9(x)$, $\delta_6(x)$, and $\delta_2(x)$. It can be seen that after adding 3 or 4 terms, the decrease of RMSE starts to level off whereas the corresponding BIC value starts to increase. By considering both criteria, we take three δ_k terms to build the final model. Thus, the chosen model is

$$v(x, F_k) = \beta(x)F_k + \delta_0(x) + \delta_{10}(x)I(k > 10) + \delta_{12}(x)I(k > 12) + \varepsilon(x, F_k). \quad [7]$$

Here, not only the initial bias $\delta_0(x)$ is significant, the systematic biases $\delta_{10}(x)$ and $\delta_{12}(x)$ also play an important role in modeling the data. To get more insights for the selected δ_k values in Eq. 7, at each stage of the selection, we define an adjusted deflection $v(x_i, F)_{\text{adj}}$ as $v(x_i, F)$ minus the selected δ_k values. For example, at stage 2, $v(x_i, F)_{\text{adj}} = v(x_i, F) - \delta_0(x) - \delta_{12}(x)I(k > 12)$. Note that the systematic bias $\delta_{12}(x)$ introduces the deflection into the image profiles starting from F_{13} , i.e., the profiles at $F = 235, 248,$ and 261 nN. Similarly, $\delta_{10}(x)$ only brings in bias on the profiles under applied force F_{11} to F_{15} . Fig. 5 shows the changes of 5 adjusted deflection profiles under applied forces F_{11} to F_{15} as the three δ_k terms are sequentially selected into the model.

The original 5 profiles are shown in Fig. 5A. When $\delta_0(x)$ is selected into the model at stage 1 of selection, it adjusts the initial bias among the 5 image profiles. In Fig. 5B, the adjusted deflection

$v(x_i, F)_{\text{adj}} = v(x_i, F) - \delta_0(x)$ looks closer to the SSBM, but the inconsistent pattern shown in Fig. 1 still remains. Note that the inconsistent pattern appears between the profiles under $F_{11} = 209$ nN and $F_{12} = 222$ nN and those under $F_{13} = 235$ nN, $F_{14} = 248$ nN, and $F_{15} = 261$ nN. At stage 2 of the selection, $\delta_{12}(x)$ is selected into the model. It further adjusts the profiles under the applied force F_{13} , F_{14} , and F_{15} . From Fig. 5C, we can see that the adjusted deflection $v(x_i, F)_{\text{adj}} = v(x_i, F) - \delta_0(x) - \delta_{12}(x)I(k > 12)$ is to push the profiles under the applied force F_{13} , F_{14} , and F_{15} to lie below those obtained at force F_{11} and F_{12} . The inconsistency no longer exists in Fig. 5C. Therefore, adding $\delta_{12}(x)$ can remove the inconsistent pattern.

At stage 3 of the selection, $\delta_{10}(x)$ is chosen into the model. It can again adjust the 5 image profiles at the applied forces from $F_{11} = 209$ nN to $F_{15} = 261$ nN. As shown in Fig. 5B, to adjust the inconsistency among these 5 profiles, it is likely that the adjusted deflections have been pushed downwards too much. From Fig. 5D, we can see that adding $\delta_{10}(x)$ into the model is to pull all 5 profiles upwards and make the adjusted deflection $v(x_i, F)_{\text{adj}} = v(x_i, F) - \delta_0(x) - \delta_{12}(x)I(k > 12) - \delta_{10}(x)I(k > 10)$ a better fit to the SSBM (see Fig. 6).

We also compute R^2 to check the goodness-of-fit at each stage of model selection. The R^2 of fitting the SSBM is 85.88%, meaning that fitting the SSBM alone accounts for 85.88% of the total experimental variations. It shows that the SSBM fits the data reasonably well in one statistical sense. However, the original curves (see Fig. 1) do not look like the theoretical shape of the SSBM (see Fig. 3). SPAR can identify and filter out, term by term, the observed deviations from the SSBM. The SSBM plus the initial bias term δ_0 fits the data better with $R^2 = 94.35\%$. The fit is further enhanced by adding 2 terms δ_{12} and δ_{10} with R^2 increased to 98.81%. The improvement due to the addition of these 3 terms is also evidenced from the profiles of the adjusted deflection $v(x, F)_{\text{adj}}$ based on the selected model shown in Fig. 7. It is more consistent with the theoretical shape (see Fig. 3) of the SSBM. Therefore, the selected model Eq. 7 can provide more reliable and precise estimation of the elastic modulus E .

To gauge the performance of the selected model, using SPAR, we compare it with the MW method. The residual plots from these two approaches are shown in Fig. 8. The residuals from the MW method show some systematic patterns, which indicates that the model needs improvement. No systematic pattern is observed in the residuals based on SPAR. Clearly, the selected model performs better. It removes the inconsistent pattern discussed above, whereas the MW method does not recognize this pattern. The residuals from the SPAR method are also much smaller.

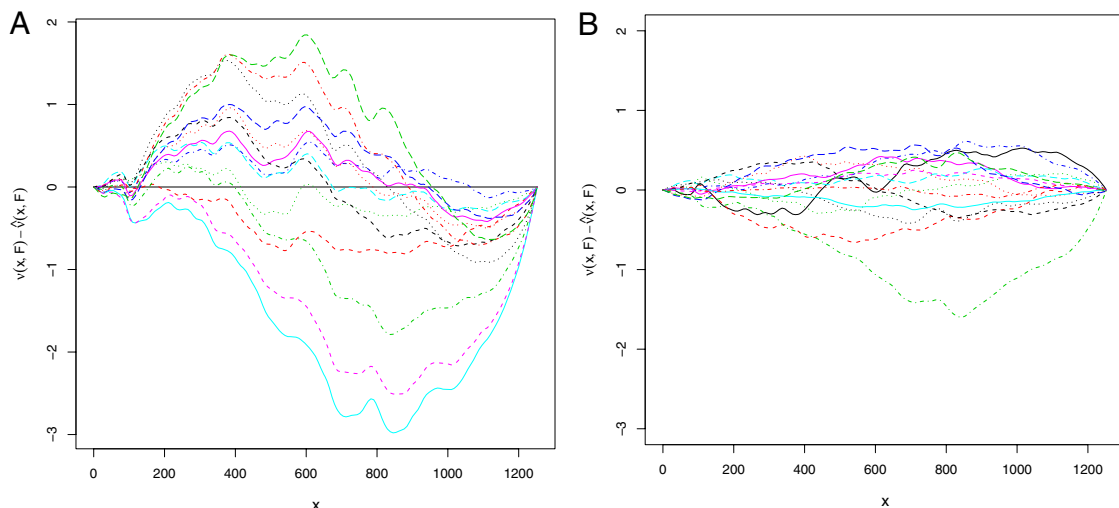


Fig. 8. Comparison of 2 methods on the NB data.

Table 1 summarizes the estimation results obtained using the two methods. Clearly SPAR gives a more precise estimate of the elastic modulus E . The standard error of E , $se(E)$, is reduced by 50%. The 95% confidence interval of E from SPAR is (99.97, 103.07), and that from the MW method is (91.24, 97.44). The nonoverlapping of intervals suggests that one of the estimates can be misleading or wrong. Because SPAR incorporates the initial bias and adjusts the inconsistent pattern in the profiles, it is expected to provide more accurate determination of the elastic modulus than the MW method. To further verify this point, we perform SPAR, using only half of the profiles of NB, i.e., the 8 profiles under the applied force $F = 78, 105, 131, 157, 183, 209, 235,$ and 261 nN. The estimate of the elastic modulus $\hat{E} = 102.67$ GPa and the 95% confidence interval (100.55, 104.79) are similar to those using SPAR with all of the 15 profiles of NB. This shows that SPAR can give a more reliable estimate even with half of the profiles. Note that the confidence interval length for half profiles using SPAR is comparable with the corresponding length for full profiles using the MW method, thus confirming the 50% reduction in $se(E)$.

Because the inconsistent pattern occurs for the last 5 image profiles, a simple alternative to SPAR, which the experimenter may favor, is to discard the last 5 profiles and apply the MW method to the first 10 profiles. The resulting estimate of the elastic modulus is 96.23 GPa. The standard error is 1.51, which is almost twice as large as the standard error from applying SPAR to the 15 profiles. This shows that adjusting the inconsistent patterns and using the complete data are better than using only the profiles with consistent pattern for estimation.

Discussion and Conclusions

In this article, we describe a method called SPAR that more precisely determines the elastic modulus of a nanobelt through statistical modeling and analysis of experimental data. It can automatically remove the initial bias and adjust the systematic artifacts and errors introduced during measurement and, thus, can give a more precise and reliable estimate of the elastic modulus.

Because of the small size of nanomaterials, the noise from the uncertainty of complex boundary conditions, instrumental instability, and the measurement environment becomes relatively large compared with the actual scale of nanomaterials. It would be difficult to conceive a physical model that can anticipate and incorporate all these sources of noise. Because the occurrence of these noises can vary from experiment to experiment, a catch-all model will be unwieldy for practical use. Statistical modeling is a more flexible and nimble alternative that can capture the noises that actually occur in an experiment. However, a purely statistical approach lacks prediction power because the identified effects in one experiment may not carry over to another. In contrast, a mechanics model with better physics can describe the intrinsic underlying properties and is thus more predictive. By avoiding the pitfalls of either approach, the proposed physical-empirical modeling approach can be a powerful tool. More discussions on this modeling and estimation technique can be found in Joseph and Melkote (10) and the references therein.

The SPAR method is proposed and its performance studied for a specific experiment on nanobelts. It can, however, have broad applications in the quantification of the mechanical properties of 1D nanomaterials. For example, San Paulo et al. (9) studied the mechanical elasticity of single and double clamped nanowires. The deflection of nanowires is measured by the controlled application of different normal forces with AFM. There is an initial variation in the growth of nanowires. Systematic bias can occur during the measurement under different applied forces. Therefore, SPAR can be used to get a better estimate of the elastic modulus. This new development demonstrates a statistical approach for quantifying the mechanical properties of 1D nanomaterials by comprehensively analyzing the acquired data and filtering out systematic artifacts.

The demonstrated methodology can be extended to other fields in nanotechnology. In the electrical measurements of nanodevices in a current range of ≈ 1 pA (10^{-12} A), a precise identification of weak signals from the noise is essential for the reliable operation of chemical and biochemical sensors to avoid false alarms. For quantum devices and single electron transistors, the measured signal may be complicated by instrumental instability and noise as well as measurement environment. In the application of piezoelectric nanowires for converting mechanical energy into electricity, the voltage generated from a nanowire depends on its dimension, the degree of its mechanical deformation, and the effectiveness of the charge output (11). A statistical evaluation of the magnitude of the output voltage is essential for understanding the efficiency of the energy conversion. For all these applications, the demonstrated methodology can be effectively applied to filter out artifacts so that the operation of the devices can be more reliable and accurate. This research can serve as an example of a new cross-interdisciplinary effort between statistics and nanotechnology.

Materials and Methods

Materials. The ZnO NBs were synthesized by a high temperature physical vapor deposition method inside a tube furnace (12). The NBs have a rectangular cross-section generally with 30–200 nm in width and thickness and 3–30 μm in length when controlling experimental parameters.

SEM imaging. A commercial scanning electron microscope (LEO 1530) was used to determine the morphology of ZnO NBs and the lateral dimensions of NBs and trenches.

AFM imaging and force measurement. A commercial atomic force microscope (Asylum Research MFP3D) was used for imaging and force measurement. AFM image provided a reliable measurement of the thickness of the NBs. The force measurement was made by scanning the NB along its length direction, using an AFM tip in contact mode at a constant applied force. A series of bending images of the NB were recorded by increasing the magnitude of the contact force. The AC240 cantilevers (spring constant of ≈ 2 N/m) from Asylum Research were used in our research, and each cantilever was carefully calibrated so that the AFM contact forces can be calculated.

ACKNOWLEDGMENTS. We thank the referees for helpful comments. The research is supported by National Science Foundation Grants DMS-0706436 and CMMI-0620259.

1. Wong EW, Sheehan PE, Lieber CM (1997) Elasticity, strength and toughness of nanorods and nanotubes. *Science* 277:1971–1975.
2. Yu MF, et al. (2000) Strength and breaking mechanism of multiwalled carbon nanotubes under tensile load. *Science* 287:637–640.
3. Poncharal P, Wang ZL, Ugarte D, de Heer WA (1999) Electrostatic deflections and electromechanical resonances of carbon nanotubes. *Science* 83:1513–1516.
4. Mai W. J. and Wang, Z.L (2006). Quantifying the elastic deformation behavior of bridged nanobelts. *Appl Phys Lett* 073112.
5. Benham PP, Crawford RJ (1987) *Mechanics of Engineering Materials* (John Wiley & Sons, New York).
6. Salvétat, et al. (1999) Elastic and shear moduli of single-walled carbon nanotube ropes. *Phys Rev Lett* 82:944–947.
7. Salvétat, et al. (1999) Mechanical Properties of Carbon Nanotubes. *Appl Phys A* 69:255–260.
8. Wu B, Heidelberg A, Boland JJ (2005) Mechanical Properties of Ultrahigh-Strength Gold Nanowires. *Nat Mater* 4:525–529.
9. San Paulo A, et al. (2005). Mechanical elasticity of single and double clamped silicon nanobeams fabricated by the vapor-liquid-solid method. *Appl Phys Lett* 053111.
10. Joseph VR, Melkote SN (2009) Statistical adjustments to engineering models. *J Qual Technol*, in press.
11. Wang ZL, Song JH (2006) Piezoelectric nanogenerators based on zinc oxide nanowire arrays. *Science* 312:242–246.
12. Pan ZW, Dai ZR, Wang ZL (2001) Nanobelts of semiconducting oxides. *Science* 291:1947–1949.